Regular Article

Pressure Dependence of Activity and Stability of Dihydrofolate Reductases of the Deep-sea Bacterium *Moritella profunda* and *Escherichia coli*

Eiji Ohmae[a,*], Chiho Murakami[a,1], Shin-ichi Tate[a], Kunihiko Gekko[a], Kazumi Hata[b,c,2], Kazuyuki Akasaka[b,c], and Chiaki Kato[d]

[a]*Department of Mathematical and Life Sciences, Graduate School of Science, Hiroshima University, Higashi-Hiroshima, Hiroshima 739-8526, Japan*
[b]*Graduate School of Biology-Oriented Science and Technology, Kinki University, Kinokawa, Wakayama 649-6493, Japan*
[c]*High Pressure Protein Research Center, Institute of Advanced Technology, Kinki University, Kinokawa, Wakayama 649-6493, Japan*
[d]*Institute of Biogeosciences, Japan Agency for Marine-Earth Science and Technology (JAMSTEC), Yokosuka 237-0061, Japan*

[1]*Present address: Fundamental Research Division, National Research Institute of Brewing, Higashi-Hiroshima, Hiroshima 739-0046, Japan*
[2]*Present address: Global Innovation Research Organization, Ritsumeikan University, Kusatsu, Shiga 525-8577, Japan*

***To whom correspondence should be addressed:**
Department of Mathematical and Life Sciences, Graduate School of Science, Hiroshima University, Higashi-Hiroshima 739-8526, Japan
Tel/Fax: +81-82-424-7389; E-mail: ohmae@hiroshima-u.ac.jp

Abbreviations: CD, circular dichroism; DHF, dihydrofolate; DHFR, dihydrofolate reductase; ecDHFR, *Escherichia coli* DHFR; mpDHFR, *Moritella profunda* DHFR; THF, tetrahydrofolate.

Abstract

To understand the pressure-adaptation mechanism of deep-sea enzymes, we studied the effects of pressure on the enzyme activity and structural stability of dihydrofolate reductase (DHFR) of the deep-sea bacterium *Moritella profunda* (mpDHFR) in comparison with those of *Escherichia coli* (ecDHFR). mpDHFR exhibited optimal enzyme activity at 50 MPa whereas ecDHFR was monotonically inactivated by pressure, suggesting inherent pressure-adaptation mechanisms in mpDHFR. The secondary structure of apo-mpDHFR was stable up to 80 ºC, as revealed by circular dichroism spectra. The free energy changes due to pressure and urea unfolding of apo-mpDHFR, determined by fluorescence spectroscopy, were smaller than those of ecDHFR, indicating the unstable structure of mpDHFR against pressure and urea despite the three-dimensional crystal structures of both DHFRs being almost the same. The respective volume changes due to pressure and urea unfolding were −45 and −53 ml/mol at 25 ºC for mpDHFR, which were smaller (less negative) than the corresponding values of −77 and −85 ml/mol for ecDHFR. These volume changes can be ascribed to the difference in internal cavity and surface hydration of each DHFR. From these results, we assume that the native structure of mpDHFR is loosely packed and highly hydrated compared with that of ecDHFR in solution.

Key words: cavity, hydration, deep sea, dihydrofolate reductase, molecular adaptation, *Moritella profunda*.

1. Introduction

There are many microorganisms living in extreme environments (high or low temperature, high salt concentration, high or low pH, and high hydrostatic pressure), but their molecular adaptation mechanisms to such environmental conditions remain unclear. Dihydrofolate reductase (DHFR), which catalyzes NADPH-dependent reduction of dihydrofolate (DHF) to tetrahydrofolate (THF), is an excellent example for studying the molecular adaptation mechanism of microorganisms. Since THF is a precursor of the cofactor required for biosynthesis of purine nucleotides and some amino acids, DHFR mediates cell housekeeping and therefore might be a key protein for adaptation of microorganisms to their environment. In 1998, Dams *et al*. [1] and Pieper *et al*. [2] determined the crystal structure of DHFR (homo-dimer) from the hyperthermophilic bacterium, *Thermotoga maritima*, and DHFR (monomer) from the Dead Sea halophilic arcaeon, *Haloferax volcanii*, respectively. The backbone structures of these DHFRs are almost the same as those of DHFRs from mesophilic bacteria such as *Escherichia coli* [3, 4], *Lactobacillus casei* [3], *Bacillus anthracis* [5], and *Staphylococcus aureus* [6]. Recently, the crystal structures of DHFR from the deep-sea piezophilic and psychrophilic bacterium, *Moritella profunda*, which was isolated from Atlantic sediments collected off the West African coast at a depth of 2,815 m [7], were determined for the apo form and the DHFR-NADPH-methotrexate ternary complex [8]. We also determined the crystal structure

of the DHFR-$NADP^+$-folate ternary complex of this enzyme (PDB code: 2zza) and found that its structure almost overlaps with that of the same complex in *E. coli* DHFR (Figure 1). However, X-ray crystallography alone is not sufficient for elucidating the molecular mechanism enabling adaptation of DHFR to the environment, and therefore, solution structures, stability, and functions of DHFR from various extreme environments should be examined.

(Figure 1)

In previous studies [9–11], we compared the structural stability and enzyme function of DHFRs from several deep-sea bacteria and ambient atmospheric species. Two deep-sea DHFRs from *Shewanella violacea* strain DSS12 (Ryukyu Trench, depth of 5,110 m [12]) and *S. benthica* strain DB21MT-2 (Mariana Trench, depth of 10,898 m [13]) showed optimal enzyme activity at approximately 100 MPa [9, 11], despite having structural stability similar to that of DHFRs from ambient atmospheric *Shewanella* species and obviously lower than that of *E. coli* DHFR [11]. However, DHFRs from other deep-sea bacteria such as *Photobacterium profundum* strain SS9, *M. japonica* strain DSK1, and *S. benthica* strain DB6705 show pressure-sensitive activity [10, 11]. On the other hand, DHFR from *S. oneidensis* strain MR-1, collected in the Oneida Lake at atmospheric pressure [14], clearly shows pressure tolerance in enzyme activity to about 100 MPa [11]. Thus, no definite correlation has been observed between the optimal pressure for DHFR enzyme activity and

habitat pressure of the parent bacterium. Therefore, further comparative studies on the structure, stability, and function of DHFRs from deep-sea and ambient atmospheric bacteria is necessary for elucidating the molecular adaptation mechanism of this enzyme to high-pressure environments.

In the present study, we investigated the effects of pressure on the enzyme activity and structural stability of DHFR of deep-sea bacterium *M. profunda* (mpDHFR) living at a depth of 2,815 m in comparison with those of *E. coli* (ecDHFR). High pressure study is a novel approach to obtain the volume changes due to unfolding of protein and enzyme kinetics [15]. To elucidate the molecular adaptation of mpDHFR to the high-pressure environment, volumetric properties of both proteins are discussed with a focus on the internal cavity and surface hydration.

2. Materials and Methods

2.1. Cloning, Overexpression, and Purification of mpDHFR

Genomic DNA of *M. profunda* was kindly provided by Dr. Nogi of JAMSTEC. Cloning and construction of the overexpression plasmid of mpDHFR were carried out by the same methods previously used for DHFR from another deep-sea bacterium, *S. violacea* [9]. DNA sequences of the primers used for PCR amplification are 5’-AGGAACTTCCGTGATTGTTTCCATGATTGC-3’ (mpDHFR-F) and

5’-GAGGATCCCTACTTCACTCGTTCAAGTAAA-3’ (mpDHFR-R). mpDHFR was purified according to the same procedures used for other deep-sea DHFRs [10]. Whole-cell lysates and purified DHFR proteins (15 μg) were separated on a 15% SDS-PAGE gel. The concentration of mpDHFR was determined from absorbance at 280 nm using a molar extinction coefficient of 27,600 $M^{-1}cm^{-1}$, which was estimated from the fluorescence intensity of fully unfolded mpDHFR in a 6 M guanidine hydrochloride solution.

2.2. Purification of ecDHFR

ecDHFR was purified as described previously [16] and fully dialyzed against 20 mM Tris-hydrochloride (pH 8.0) containing 0.1 mM EDTA and 0.1 mM dithiothreitol before use. The protein concentration was determined from absorbance at 280 nm using a molar extinction coefficient of 31,100 $M^{-1}cm^{-1}$ [17].

2.3. Circular Dichroism Spectrometry

Far-ultraviolet circular dichroism (CD) spectra of ecDHFR and mpDHFR were measured using a J-720W spectropolarimeter (Jasco Inc., Tokyo, Japan). Temperature was maintained at 15 ºC using a Peltier-controlled thermobath (PTC-348W, Jasco Inc.). Solvent composition was 20 mM Tris-hydrochloride (pH 8.0) containing 0.1 mM EDTA and 0.1 mM dithiothreitol. This buffer was used for all experiments except for the activity measurements. Protein concentration was 10 μM.

2.4. Fluorescence Spectrometry

Fluorescence spectra of both DHFRs were measured using a FP-750 spectrofluorometer (Jasco Inc.) with an excitation wavelength of 290 nm and an emission wavelength of 300–450 nm. Temperature was maintained at 15 ºC with a circulating thermobath (NESLAB RTE-110, Thermo Fischer Scientific, Waltham, MA). The solvent was the same as in the CD measurements. Protein concentration was 0.3 and 0.5 μM for ecDHFR and mpDHFR, respectively. Spectra intensity was normalized to 1 μM protein.

2.5. High Pressure Enzyme Assay

Pressure dependence of the enzyme activity of mpDHFR was measured using a V-560 spectrophotometer (Jasco Inc.) equipped with a high-pressure spectroscopic cell unit (Syn Corporation PCI-400, Kyotanabe, Japan) and a hand pump (Syn Corporation HP-500DG) as described previously [18]. Temperature was maintained at 25 ºC with a circulating thermobath (NESLAB RTE-5, Thermo Fischer Scientific). The solvent used was 20 mM Tris-hydrochloride (pH 7.0) containing 0.1 mM EDTA and 0.1 mM dithiothreitol, 250 μM NADPH, and 250 μM DHF. Concentrations of DHF (Sigma-Aldrich, St. Louis, MO) and NADPH (Oriental Yeast, Tokyo, Japan) were determined spectrophotometrically using molar extinction coefficients of 28,000 $M^{-1}cm^{-1}$ at 282 nm and 6,200 $M^{-1}cm^{-1}$ at 339 nm, respectively [19]. The enzyme reaction was started by mixing the DHF solution with the enzyme solution containing NADPH at final concentrations of 1–2 nM DHFR. The initial velocity of the enzyme reaction was calculated from the time course of absorbance at 370

nm with a differential molar extinction coefficient at each pressure (e.g., 3,180 and 3,710 M^{-1} cm^{-1} at 0.1 and 250 MPa, respectively) [18]. The initial velocity of double independent measurements was averaged for each pressure. The activation free energy (ΔG^*) and the activation volume (ΔV^*) of the enzyme reaction were calculated according to the following equation, which is applicable to the saturated substrate concentrations [18]:

$$\Delta V^* = \partial \Delta G^* / \partial P = \partial(-RT \ln k_{cat}) / \partial P = \partial(-RT \ln v) / \partial P \quad (1)$$

where R is the gas constant, T is temperature, P is pressure, and v is the initial velocity of the enzyme reaction.

2.6. Thermal Unfolding

Thermal unfolding of both DHFRs was monitored by CD measurements using a 1-mm path length cell. Temperature was increased at a rate of 45 ºC·h^{-1} using a PTC-348W Peltier-controlled heat block (Jasco Inc.) and monitored with a thermistor placed in the heating block. Protein concentration and solvent composition were the same as those for the CD measurements in Section *2.3*. The reversibility of thermal unfolding of both DHFRs was examined by measuring enzyme activity at 25 ºC before and after incubation at 65 ºC for 10 min.

2.7. Pressure Unfolding

Pressure unfolding of both DHFRs was monitored by fluorescence spectra using a FP-750 spectrofluorometer (Jasco Inc.) equipped with the same high-pressure system

used for the activity measurements. Excitation wavelength was 290 nm and emission wavelength was 300–450 nm. Temperature was maintained with a circulating thermobath (NESLAB RTE-110) and monitored with a sensor inserted directly into the sample solution after decompression. Concentration of ecDHFR and mpDHFR was 3 and 5 μM, respectively. Protein solutions were equilibrated for 30 min at each pressure before the fluorescence spectra were measured. Reversibility of pressure unfolding was confirmed to be >95 % from the spectra after decompression. A center of fluorescence spectral mass, *CSM*, was calculated according to the following equation,

$$CSM = \sum \lambda_i F_i / \sum F_i \quad (2)$$

where λ_i and F_i are the wavenumber represented in cm^{-1} and fluorescence intensity, respectively, at wavelength *i* [20]. The obtained *CSM* data were directly fitted to the two-state unfolding model, native (N) ⇔ unfolded (U), by nonlinear least-squares regression analysis as follows:

$$y_{obs} = \{ y_N + y_U \exp(-\Delta G_u / RT)\} / \{1 + \exp(-\Delta G_u / RT)\} \quad (3)$$

where ΔG_u is the change in Gibbs free energy due to unfolding, and y_N and y_U are the *CSM* values of the native and unfolded forms, respectively. y_N and y_U at a given pressure were estimated by assuming the same linear dependence in the transition region as in the pure native (pre-transition region) and unfolded states (post-transition region). The pressure dependence of the Gibbs free energy change was calculated as follows:

$$\Delta G_u = \Delta G^o_P + P\Delta V_P \quad (4)$$

where ΔG^o_P is the Gibbs free energy change of unfolding at 0 MPa and ΔV_P is the partial molar volume change due to pressure unfolding. ΔG^o_P can be regarded as the Gibbs free energy change at atmospheric pressure, since the pressure difference of 0.1 MPa is negligibly small in this experiment. The pressure at the midpoint of the transition ($\Delta G_u = 0$) is defined as P_m.

2.8. Urea Unfolding at Atmospheric Pressure

Equilibrium unfolding of both DHFRs induced by urea (ultra pure product, MP Biomedicals, Solon, OH) was monitored at 25 ºC by the molar ellipticity at 222 nm, $[\theta]_{222}$, and the fluorescence spectra as described previously [16, 11]. Protein concentration was about 20 and 1 μM for CD and fluorescence measurements, respectively. All samples were fully equilibrated for 24 h at each denaturant concentration before measurement of CD and fluorescence. The observed $[\theta]_{222}$ and *CSM* values (41 points) were fitted directly to the two-state unfolding model (equation 3) to calculate the Gibbs free energy change due to urea unfolding, ΔG_u. Urea concentration dependence of ΔG_u was calculated as follows [21]:

$$\Delta G_u = \Delta G^o_U - m\,[\text{urea}] \quad (5)$$

where ΔG^o_U is the Gibbs free energy change due to unfolding in the absence of denaturant, and the slope, *m*, is the parameter reflecting the cooperativity of the transitions. The urea concentration at the midpoint of the transition is defined as C_m.

2.9. Pressure Dependence of Urea Unfolding

Pressure dependence of urea unfolding was monitored by fluorescence spectra of DHFR solutions under various urea concentrations and pressures as described above. The concentration of ecDHFR and mpDHFR was 3 and 5 μM, respectively. Protein solutions were equilibrated for 24 h at each urea concentration and for 10 min at 0.1, 50, 100, 150, 200, and 250 MPa before fluorescence measurement. *CSM* values calculated from the spectra were plotted against urea concentration at each pressure and fitted to equations 3 and 5. The obtained ΔG^{o}_{U} values were plotted against pressure, P, to calculate the volume change due to urea unfolding, ΔV_U, as follows:

$$\Delta G^{o}_{U} = \Delta G^{o}_{UP} + P\Delta V_U \quad (6)$$

where ΔG^{o}_{UP} is the Gibbs free energy change due to unfolding in the absence of urea at 0 MPa (substantially at atmospheric pressure).

3. Results

3.1. Structure of mpDHFR

The purified mpDHFR protein showed a single band on SDS-PAGE gel (Figure 2). Mass spectroscopic and crystallographic data indicated that this protein had no additional residues in the N-terminal region unlike other deep-sea DHFRs previously reported [10, 11], enabling us to directly compare this protein with ecDHFR.

(Figure 2)

Recently, we determined the crystal structure of the mpDHFR-$NADP^+$-folate ternary complex (PDB code: 2zza) and found that the backbone structure of mpDHFR almost overlaps with that of ecDHFR in the same ternary complex (Figure 1). The solution structure of both DHFRs was compared using far-ultraviolet CD spectra in the presence and absence of NADPH or DHF at 15 ºC and pH 8.0 (Figure 3A). The CD spectrum of apo-mpDHFR showed a similar peak intensity to that of ecDHFR but clearly blue-shifted to 207 nm with a shoulder around 215 nm. The different CD spectra do not necessarily mean a difference in the secondary structures of both DHFRs but would be ascribed to breaking the Trp47–Trp74 exciton coupling in ecDHFR [22], because the two tryptophan residues are substituted by phenylalanine and valine in mpDHFR, and the CD spectrum of ecDHFR was significantly affected by substitution of tryptophan residues [23]. Single amino acid substitutions at other residues could also affect the CD spectrum of DHFR without perturbation of the secondary structure [16, 24, 25]. On the other hand, Evans *et al*. reported that the CD spectrum of apo-mpDHFR has two small peaks, one positive and one negative, of almost the same intensity (around 290 and 270 nm, respectively) [26], but we could not observe such peaks (Figure S1). The reported peaks may be due to a cofactor remaining in the sample solution because the peak intensities are too large for the CD signals from aromatic side chains, and the CD spectrum of $NADP^+$ had similar peaks

around the corresponding wavelengths (Figure S1). In the present study, the CD spectrum of mpDHFR was compared in the presence and absence of NADPH or DHF as shown in Figure 3A. Evidently, the CD spectrum of mpDHFR red-shifted to 211 and 212 nm in the presence of NADPH and DHF, respectively, and the shoulder disappeared without affecting peak intensity. These results suggest that the structure of mpDHFR is slightly modified by binding of ligands in solution.

(Figure 3)

The tertiary conformation of both DHFRs was further confirmed by fluorescence spectra at 15 ºC and pH 8.0 (Figure 3B). mpDHFR showed a smaller peak intensity than ecDHFR as expected from the smaller number of Trp residues in mpDHFR (three) than that in ecDHFR (five). The peak wavelengths for mpDHFR and ecDHFR at 0.1 MPa were 343 and 345 nm, respectively, which were shorter than the wavelength of buried Trp residues (~335 nm). This result suggests that the Trp residues of both proteins are partially hydrated at 0.1 MPa, with Trp residues of mpDHFR being in slightly more hydrophobic environments than those of ecDHFR. From the CD and fluorescence spectra, we have detected no notable differences in the secondary and tertiary structures between mpDHFR and ecDHFR in solution.

3.2. Pressure Effect on Enzyme Activity

To characterize the enzymatic function of deep-sea DHFRs, the pressure dependence

of enzyme activity of mpDHFR was examined at 25 ºC and pH 7.0. As shown in Figure 4A, the enzyme activity of mpDHFR increased to 120% at 50 MPa as pressure increased and decreased rapidly to 45% with further increasing pressure to 250 MPa, which is a similar response to the results of Hay *et al*. [8]. On the other hand, the enzyme activity of ecDHFR monotonically decreased as the pressure increased to 250 MPa [10, 18]. Therefore, mpDHFR seemed to exhibit a pressure-adaptation mechanism.

The apparent activation free energy of the enzyme reaction was calculated by equation 1 and plotted against pressure in Figure 4B, from which activation volume, ΔV^*, was obtained as listed in Table 1. The ΔV^* values of mpDHFR were –8.6 and 8.6 ml/mol below and above 50 MPa, respectively. These values were comparable to those of deep-sea DHFRs from *S. violacea* (–8.6 and 5.6 ml/mol) and *S. benthica* strain DB21MT-2 (–3.5 and 6.5 ml/mol), suggesting a similar pressure-adaptation mechanism of these piezophilic DHFRs at relatively low pressure [11].

(Figure 4) (Table 1)

3.4. Thermal Unfolding

The thermal stability of ecDHFR and mpDHFR without ligands was evaluated from the temperature dependence of far-ultraviolet CD spectra at pH 8.0 and atmospheric pressure. As shown in Figure 5A, while the molar ellipticity of ecDHFR around 220 nm increased with increasing temperature, that of mpDHFR decreased (became more negative) (Figure 5B).

The $[\theta]_{222}$ values of ecDHFR and mpDHFR were plotted against temperature (Figure 5B, inset). Evidently, mpDHFR showed abnormal behavior whereby the secondary structure increased with increasing temperature, although ecDHFR followed a three-state unfolding model as reported previously [27]. On the other hand, Evans *et al*. reported that molar ellipticity at 222 nm conversely increases (becomes less negative) with temperature due to thermal unfolding at 30–40 ºC [26]. A possible explanation for this discrepancy is that the temperature dependence of the molar ellipticity might be caused by not disruption of the secondary structure, but dissociation of the coexisting cofactor as mentioned in Section 3.1 and shown in Figure S1. This is supported by the fact that the CD spectrum of mpDHFR at 65 ºC in the report of Evans *et al.* shows a clear positive peak around 195 nm where the random coil structure should have a large negative peak [28], reflecting the considerable amount of remaining secondary structures, and that enzyme activity significantly decreases after heating at 65 ºC for 10 min (data not shown), as reported by Xu *et al*. [29].

This abnormal thermal transition of mpDHFR cannot be explicitly explained at present. Aggregation of protein would generally reduce the CD intensity due to the decrease in concentration of soluble protein overall the wavelength region observed, but there appears an isoellipticity point around 210 nm in CD spectra of mpDHFR as well as ecDHFR (Fig. 5). This result suggests that some conformation change or association of mpDHFR occurs at high temperature because the small soluble aggregates or oligomers such as protofibrils

are known to increase CD intensity [30, 31]. Similar temperature dependence of CD spectra was observed for other deep-sea DHFRs from *S. violacea* and *P. profundum* (data not shown), hence this abnormal temperature dependence of CD may be a common character of deep-sea DHFRs. However, this abnormal thermal stability is not the result of adaptation to low deep-sea temperature (1–4 ºC), because the optimal growth temperature of *M. profunda* is 2 ºC [7]. Therefore, psychrophilic bacteria would not necessarily contain only psychrophilic proteins on the analogy of our finding that enzymes of piezophilic bacteria are not necessarily piezophilic [10, 11].

(Figure 5)

3.5. Pressure Unfolding

The pressure unfolding of ecDHFR and mpDHFR without ligands was examined by fluorescence spectra at pH 8.0 and various temperatures (Figure 6). The *CSM* value of ecDHFR showed a clear transition in the pressure region from 200 to 400 MPa, shifting slightly to the higher pressure as the temperature decreased (Figure 6A). On the other hand, the *CSM* value of mpDHFR decreased rapidly with increasing pressure below 200 MPa (Figure 6B), and the transition shifted to lower pressure with an increased cooperativity as temperature decreased. These results clearly indicate that mpDHFR is less stable against pressure than ecDHFR despite mpDHFR being obtained from a deep-sea bacterium.

The *CSM* values were fitted to equations 3 and 4 to calculate thermodynamic parameters. There was a good linear correlation between the calculated ΔG_u values and pressure as shown in the inset of Figure 7, enabling us to determine the Gibbs free energy change due to unfolding at 0.1 MPa (ΔG^o_P), the volume change of pressure unfolding (ΔV_P), and the midpoint pressure of the transition (P_m). As listed in Table 2, the ΔG^o_P values of mpDHFR (2.9–3.3 kJ/mol) were far smaller than those of ecDHFR (16.5–21.5 kJ/mol), indicating the lower structural stability of mpDHFR. The obtained ΔV_P values of mpDHFR, −(40–50) ml/mol, were less negative than those of ecDHFR, − (64–79) ml/mol, suggesting a smaller conformational change of mpDHFR. The temperature dependence of ΔG^o_P and ΔV_P values is opposite for ecDHFR and mpDHFR in the temperature range examined, although the P_m values were not dependent on the temperature within experimental error, suggesting different maximal-stability temperatures of both DHFRs. These ΔG^o_P values are smaller than those for the mpDHFR-folate complex (15.8 ± 4.1 kJ/mol), which was estimated at 15 ºC by high-pressure NMR experiments [32], whilst the ΔV_P values are comparable with those for this complex (−66 ± 19 ml/mol). These results suggest that folate binding significantly enhances the stability of mpDHFR whereas it has no substantial influence on the volume change, probably due to the small partial molar volume of folate compared with that of the protein.

(Figure 6) (Table 2)

3.6. Urea Unfolding under High Pressures

Before the high pressure study, urea unfolding of mpDHFR and ecDHFR without ligands was examined with CD and fluorescence spectra at 25 ºC and pH 8.0 at atmospheric pressure. As shown in Figure 7, the $[\theta]_{222}$ and *CSM* values showed the transitions at the lower urea concentration for mpDHFR than for ecDHFR, indicating the less stable structure of mpDHFR. The $[\theta]_{222}$ and *CSM* values were thoroughly fitted to the transition curves calculated with equations 3 and 5, confirming that urea unfolding of both DHFRs follows a two-state unfolding model. The calculated Gibbs free energy change due to unfolding in the absence of urea (ΔG^{o}_{U}), cooperativity of the transition (*m*), and the midpoint urea concentration of the transition (C_m) are listed in Table 3. These values obtained by CD are in agreement with those obtained by fluorescence within experimental error, demonstrating that the fluorescence method is applicable for examining the pressure effect on urea unfolding. The ΔG^{o}_{U} value for mpDHFR, 7.6 ± 0.8 kJ/mol, is smaller than the previously reported value, 13.4 kJ/mol, which was measured under different conditions (15 ºC and pH 7.0 in a phosphate buffer) [30], but close to that (7.9–8.7 kJ/mol) for other three deep-sea DHFRs from *Shewanella* species at 15 ºC in the same buffer [11]. However, these ΔG^{o}_{U} values are significantly smaller than those for ecDHFR, 22.5 ± 2.3 kJ/mol, suggesting that deep-sea DHFRs are commonly unstable compared with ecDHFR. Furthermore, the small *m* value for mpDHFR indicates that the unfolding transition of this protein is less

cooperative than ecDHFR.

(Figure 7) (Table 3)

To estimate the volume change due to urea unfolding, we examined the urea concentration dependence of the *CSM* values of both DHFRs under various pressures at 25 ºC and pH 8.0. As shown in Figure 8, the transition curves of both DHFRs shifted to the lower urea concentration with increasing pressure, indicating the significant destabilization of the structures by pressure. The thermodynamic parameters, ΔG°_{U}, m, and C_m, were calculated by fitting the *CSM* values to equations 3 and 5 at various pressures except for 200 and 250 MPa for mpDHFR. The *CSM* values for the native state of mpDHFR at 100 and 150 MPa were assumed to be identical to those calculated for the pressure-induced unfolding. The ΔG°_{U} and C_m values (Table 3) decreased with increasing pressure, that is, high pressure destabilized the structure of both DHFRs, which is consistent with the results of the pressure-unfolding experiments (Figure 6 and Table 2). The m value decreased with increasing pressure, indicating the diminished cooperativity of the transition under high pressure. From the slopes of the ΔG°_{U}–P plots (Equation 6; Figure 8B, inset), the volume change due to urea unfolding, ΔV_U, was estimated to be −85 ± 7 ml/mol and −53 ± 7 ml/mol for ecDHFR and mpDHFR, respectively. This result suggests that the urea-induced conformational change is smaller for mpDHFR than for ecDHFR, which is consistent with the results from pressure unfolding (ΔV_P). These ΔV_U values are slightly larger (more

negative) than the ΔV_P values of the corresponding DHFR obtained for the pressure unfolding (Table 2). This is reasonable because in general, proteins are more extensively unfolded by urea than by pressure, but the small difference between ΔV_U and ΔV_P suggests that the pressure-unfolded state of both DHFRs is close to the urea-unfolded one.

(Figure 8)

4. Discussion

The enzymatic function and structural stability of mpDHFR are significantly different from those of ecDHFR, although the crystal and solution structures of both DHFR are almost the same. The enzyme activity of mpDHFR is higher under moderately high pressure relative to atmospheric pressure, although the activity of ecDHFR monotonically decreases with pressure. The thermal stability of mpDHFR is higher than that of ecDHFR in the secondary structure, but Gibbs free energy (ΔG^o_P and ΔG^o_U) and volume changes (ΔV_P and ΔV_U) due to pressure and urea unfolding of mpDHFR are smaller than those of ecDHFR. Elucidation of these findings will give new insight into the molecular adaptation mechanisms of proteins to the high-pressure conditions of the deep sea and other extreme environments.

4.1. Effect of Pressure on Function of mpDHFR

As shown in Figure 4A, pressure dependence of the enzyme activity of mpDHFR is

biphasic: the change in sign of ΔV^* above and below 50 MPa suggests shifts in the rate-limiting step of the enzyme reaction. This behavior was also observed for other deep-sea DHFRs of *S. violacea* and *S. benthica* strain DB21MT-2 [9–11]. However, the pressure dependence of the enzyme activity of deep-sea DHFRs is not simple and depends on the parent bacteria and amino acid sequences. Three deep-sea DHFRs from *S. banthica* strain DB6705, *P. profundum*, and *M. japonica* showed monotonic decrease of enzyme activity by pressure, and another deep-sea DHFR from *M. yayanosii* showed almost constant activity up to 75 MPa [10, 11]. Such pressure tolerance was also observed for DHFR from *S. oneidensis*, which live under ambient atmospheric pressure [11]. Further, Dreyfus *et al.* reported that the pressure dependence of enzyme activity of mammalian mitochondrial ATPase is biphasic [33]. Therefore, the biphasic pressure dependence of the activity of mpDHFR might not necessarily result from its adaptation to the high-pressure environment, but rather incidentally from the different amino acid sequences. In general, an enzyme reaction includes many pressure-dependent processes with different activation volumes, leading to characteristic pressure dependence of or optimal pressure for enzyme activity. The enzyme kinetics of ecDHFR consists of at least five elementary processes; two binding steps of cofactor (NADPH) and substrate (DHF), hydride transfer step, and two releasing steps of products ($NADP^+$ and THF). It is probable that the enzyme kinetics of mpDHFR as well as those of other deep-sea DHFRs follow those of ecDHFR, judging from

the conserved amino acid residues in the active site. In such processes, the release of product (THF) is the rate-limiting step for ecDHFR at atmospheric pressure [17]. We found that the hydride transfer of ecDHFR is not the rate-limiting process under high pressure and predicted three candidates for the rate-limiting process: two are the releasing processes of THF and $NADP^+$, and one is the conformational change of the enzyme [18]. The hydride transfer is also known not to be the rate-limiting process for mpDHFR under high pressure [8]. Considering the comparable ΔV^* values and the pressure-tolerant behavior of enzyme activity, any of the three candidates could be the rate-limiting process for mpDHFR as well as other deep-sea DHFRs [10, 11]. Understanding the pressure-tolerant function of deep-sea DHFRs must be preceded by detailed stopped-flow analysis of enzyme kinetics under high pressure and high pressure NMR analysis of enzyme structure.

4.2. Effect of Pressure on Stability of mpDHFR

The free energy and volume changes due to unfolding are important measures of the stability and structure of a protein, although they are only the difference between the corresponding partial quantities in the native and unfolded states. The smaller ΔG°_{P} and ΔG°_{U} values of mpDHFR (Tables 2 and 3) clearly indicate that the structural stability of mpDHFR against pressure and urea is lower than that of ecDHFR, although the three-dimensional backbone structure of both DHFRs is almost the same (Figure 1). The smaller ΔV_P and ΔV_U values of mpDHFR also suggest that its pressure- and urea-induced

conformational changes are not very large compared with ecDHFR. The relationship of $\Delta G^{o}_{P} < \Delta G^{o}_{U}$ to $\Delta V_{P} < \Delta V_{U}$ for both DHFRs is consistent with the general idea that urea and guanidine hydrochloride are strong denaturants for inducing large conformational changes in protein compared with pressure and thermal unfolding. However, the values of ΔG^{o}_{P} and ΔV_{P} are about 90% the ΔG^{o}_{U} and ΔV_{U} values of ecDHFR, suggesting that the pressure-unfolded structure might be close to the urea-unfolded one. Such a large conformational change by pressure is also expected for mpDHFR since the ΔV_{P} value is about 80% of ΔV_{U}. Although this is not clearly recognized at the free energy level, the comparable difference between ΔG^{o}_{P} and ΔG^{o}_{U} for mpDHFR and ecDHFR suggests a similarity in the pressure- and urea-unfolded structures of mpDHFR. In general, the unfolded state is an ensemble of various structures of protein, and even the native state includes the unfolded structures although their populations are very small. Judging from the ΔG^{o}_{P} (2.9–3.3 kJ/mol) and ΔG^{o}_{U} (7.6–7.9 kJ/mol) values for mpDHFR, about 23 % of the pressure-unfolded structure and 4% of the urea-unfolded structure may coexist in the native state of this protein at 25 ºC and atmospheric pressure. However, this result does not necessarily contradict a two-state unfolding model, since the model is based on two states and does not assume two structures.

The volume changes due to unfolding are directly related to the pressure effects on the structure of deep-sea proteins. It is noteworthy that the difference between ΔV_{P} and ΔV_{U}

($\Delta V_U - \Delta V_P$) is about −8 ml/mol for both mpDHFR and ecDHFR since ΔV_P is estimated to be −45 and −77 ml/mol at 25 ºC for mpDHFR and ecDHFR, respectively, by interpolating the temperature dependence of ΔV_P (Table 2). Although these estimates involves the large experimental errors, this difference suggests that the transition from pressure-unfolded to urea-unfolded states is similar for both DHFRs and hence the difference in ΔV_U can be ascribed mainly to the volume change from the native to the pressure-unfolded state of each DHFR. If this is the case, the smaller volume change of mpDHFR would be due mainly to its small partial molar volume in the native state compared with that of ecDHFR, since the unfolded states due to urea and pressure would not be largely different between the DHFRs.

The partial molar volume (V^o) of a protein in water is determined by the following three factors: constitutive atomic volume (V_c), cavity resulting from imperfect atomic packing (V_{cav}), and volume change due to hydration (ΔV_{sol}) [15, 34, 35]:

$$V^o = V_c + V_{cav} + \Delta V_{sol} \quad (7)$$

Since the constitutive atomic volume is unchangeable before and after unfolding, the volume change due to unfolding (ΔV_P or ΔV_U) results from the modified internal cavity and surface hydration as follows:

$$\Delta V_P \text{ or } \Delta V_U = V^o \text{ (unfolded)} - V^o \text{ (native)} = \Delta V_{cav} + \Delta\Delta V_{sol} \quad (8)$$

Cavities contribute positively, and hydration contributes negatively to V^o, and hence the

experimentally observed negative values of ΔV_P and ΔV_U can be ascribed to the decrease in cavity and/or the increase in hydration due to unfolding.

Although it is difficult to distinguish the contributions of cavity and surface hydration, the V_{cav} of a native protein can be estimated from its X-ray structure by rolling a probe sphere around an internal atomic surface using the program MOLMOL (http://www.mol.biol.ethz.ch/wuthrich/software/molmol). In the present study, the V_{cav} values of mp DHFR (PDB ID: 2zza) and ecDHFR (PDB ID: 1rx2) without ligands were estimated at 340 and 270 $Å^3$, respectively, with a probe size of 1.0 Å giving the maximum value of the cavities. On the other hand, the accessible surface areas of mpDHFR without ligands calculated by the GetArea server (http://curie.utmb.edu/getarea.html) [36] were estimated to be 8633 $Å^2$ with a probe size of 1.4 Å, which is slightly larger than that (8542 $Å^2$) of ecDHFR. These results suggest that the smaller V^o of mpDHFR than that of ecDHFR could result from the enhanced surface hydration being dominant over the cavity effect in the native structure. Thus, mpDHFR is expected to take on a loosely packed and highly hydrated structure in solution, compared with ecDHFR. There is some indirect evidence for this hypothesis. Significant pressure and urea-concentration dependences of the fluorescence spectra of mpDHFR in the native state (Figures 6 and 7) suggest easy accession of solvent molecules to the tryptophan side chains located on the inside of the protein molecule. Abnormal thermal stability of mpDHFR (Figure 5) also supports the

enhanced hydration in the native structure, which reduces the heat capacity change due to thermal unfolding. Since both the cavity and surface hydration are sensitive to amino acid side chains, mpDHFR is able to adapt to the high-pressure environment of the deep sea without major changes to its backbone structure.

Investigation of mpDHFR revealed the characteristic effect of pressure on stability and enzyme activity, which was different from that of ecDHFR. The proposed hypothesis for the adaptation of mpDHFR to pressure should be confirmed by further detailed structural and functional analyses. Direct measurements of partial specific volume and compressibility of deep-sea DHFRs (currently in progress) will provide the key for solving the molecular adaptation mechanisms of deep-sea protein.

Acknowledgement

This work was financially supported by a Grant-in-Aid for Scientific Research (No. 16657031 for K.G.) and by the Academic Frontier Program (07F010 for K.A.) from the Ministry of Education, Science, Sports and Culture of Japan.

References

[1] T. Dams, G. Bohm, G. Auerbach, G. Bader, H. Schurig, R. Jaenicke, Homo-dimeric recombinant dihydrofolate reductase from *Thermotoga maritima* shows extreme intrinsic stability, Biol. Chem. 379 (1998) 367–371.

[2] U. Pieper, G. Kapadia, M. Mevarech, O. Helzberg, Structural features of halophilicity derived from the crystal structure of dihydrofolate reductase from the Dead Sea halophilic archaeon, *Haloferax volcanii*, Structure 15 (1998) 75–88.

[3] J.T. Bolin, D.J. Filman, D.A. Matthews, R.C. Hamlin, J. Kraut, Crystal structures of *Escherichia coli* and *Lactobacillus casei* dihydrofolate reductase refined at 1.7 Å resolution. I. General features and binding of methotrexate, J. Biol. Chem. 257 (1982) 13650–13662.

[4] M.R. Sawaya, J. Kraut, Loop and subdomain movements in the mechanism of *Escherichia coli* dihydrofolate reductase: crystallographic evidence, Biochemistry 36 (1997) 586–603.

[5] B.C. Bennett, H. Xu, R.F. Simmerman, R.E. Lee, C.G. Dealwis, Crystal structure of the anthrax drug target, *Bacillus anthracis* dihydrofolate reductase, J. Med. Chem. 50 (2007) 4374–4381.

[6] K.M. Frey, J. Liu, M.N. Lombardo, D.B. Bolstad, D.L. Wright, A.C. Anderson, Crystal structures of wild-type and mutant methicillin-resistant *Staphylococcus aureus*

dihydrofolate reductase reveal an alternate conformation of NADPH that may be linked to trimethoprim resistance, J. Mol. Biol. 387 (2009) 1298–1308.

[7] Y. Xu, Y. Nogi, C. Kato, Z. Liang, H.J. Rüger, D. De Kegel, N. Glansdorff, *Moritella profunda* sp. nov. and *Moritella abyssi* sp. nov., two psychropiezophilic organisms isolated from deep Atlantic sediments, Int. J. Syst. Evol. Microbiol. 53 (2003) 533-538.

[8] S. Hay, R.M. Evans, C. Levy, E.J. Loveridge, X. Wang, D. Leys, R.K. Allemann, N.S. Scrutton, Are the catalytic properties of enzymes from piezophilic organisms pressure adapted? Chembiochem 10 (2009) 2348–2353.

[9] E. Ohmae, K. Kubota, K. Nakasone, C. Kato, K. Gekko, Pressure-dependent activity of dihydrofolate reductase from a deep-sea bacterium *Shewanella violacea* strain DSS12, Chem. Lett. 33 (2004) 798–799.

[10] C. Murakami, E. Ohmae, S. Tate, K. Gekko, K., Nakasone, C. Kato, Cloning and characterization of dihydrofolate reductases from deep-sea bacteria, J. Biochem. 147 (2010) 591–595.

[11] C. Murakami, E. Ohmae, S. Tate, K. Gekko, K. Nakasone, C. Kato, Comparative study on dihydrofolate reductases from *Shewanella* species living in deep-sea and ambient atmospheric environments, Extremophiles 15 (2011) 165–175.

[12] C. Kato, T. Sato, K. Horikoshi, Isolation and properties of barophilic and barotolerant bacteria from deep-sea mud samples, Biodiversity and Conservation 4 (1995) 1–9.

[13] C. Kato, L. Li, Y. Nogi, Y. Nakamura, J. Tamaoka, K. Horikoshi, Extremely barophilic bacteria isolated from the Mariana Trench, Challenger Deep, at a depth of 11,000 meters, Appl. Environ. Microbiol. 64 (1998) 1510–1513.

[14] K. Venkateswaran, D.P. Moser, M.E. Dollhopf, D.P. Lies, D.A. Saffarini, B.J. MacGregor, D.B. Ringelberg, D.C. White, M. Nishijima, H. Sano, J. Burghardt, E. Stackebrandt, K.H. Nealson, Polyphasic taxonomy of the genus *Shewanella* and description of *Shewanella oneidensis* sp. nov., Int. J. Syst. Bacteriol. 49 (1999) 705–724.

[15] C. Balny, P. Masson, K. Heremans Eds. Frontiers in high pressure biochemistry and biophysics. Biochim. Biophys. Acta 1595 (1–2) (2002).

[16] E. Ohmae, K. Iriyama, S. Ichihara, K. Gekko, Effects of point mutations at the flexible loop glycine-67 of *Escherichia coli* dihydrofolate reductase on its stability and function, J. Biochem. 119 (1996) 946–953.

[17] C.A. Fierke, K.A. Johnson, S.J. Benkovic, Construction and evaluation of the kinetic scheme associated with dihydrofolate reductase from *Escherichia coli*, Biochemistry 26 (1987) 4085–4092.

[18] E. Ohmae, M. Tatsuta, F. Abe, C. Kato, N. Tanaka, S. Kunugi, K. Gekko, Effects of pressure on enzyme function of *Escherichia coli* dihydrofolate reductase, Biochim. Biophys. Acta 1784 (2008) 1115–1121.

[19] R.M.C. Dawson, D.C. Elliot, W.H. Elliot, K.M. Jones, Data for Biochemical Research,

(1969) Oxford University Press, Oxford.

[20] G.J.A. Vidugiris, C.A. Royer, Determination of the volume changes for pressure-induced transitions of apomyoglobin between the native, molten globule, and unfolded states, Biophysical J. 75 (1998) 463–470.

[21] C.N. Pace, Determination and analysis of urea and guanidine hydrochloride denaturation curves, In: C.H.W. Hirs, S.N. Timasheff (eds) Methods in Enzymology Vol. 131 (1985) Academic Press, New York, pp 267–280.

[22] K. Kuwajima, E.P. Garvey, B.E. Finn, C.R. Matthews, S. Sugai, Transient intermediates in the folding of dihydrofolate reductase as detected by far-ultraviolet circular dichroism spectroscopy, Biochemistry 30 (1991) 7693–7703.

[23] E. Ohmae, Y. Sasaki, K. Gekko, Effects of five-tryptophan mutations on structure, stability and function of *Escherichia coli* dihydrofolate reductase, J. Biochem. 130 (2001) 439–447.

[24] K. Gekko, Y. Kunori, H. Takeuchi, S. Ichihara, M. Kodama, Point mutations at glycine-121 of *Escherichia coli* dihydrofolate reductase: important roles of a flexible loop in the stability and function, J. Biochem. 116 (1994) 34–41.

[25] E. Ohmae, Y. Fukumizu, M. Iwakura, K. Gekko, Effects of mutation at methionine-42 of *Escherichia coli* dihydrofolate reductase on stability and function: implication of hydrophobic interactions, J. Biochem. 137 (2005) 643–652.

[26] R.M. Evans, E.M. Behiry, L.H. Tey, J. Guo, E.J. Loveridge, R.K. Allemann. Catalysis by dihydrofolate reductase from the psychropiezophile *Moritella profunda*, Chembiochem 11 (2010) 2010–2017.

[27] E. Ohmae, T. Kurumiya, S. Makino, K. Gekko, K. Acid and thermal unfolding of *Escherichia coli* dihydrofolate reductase, J. Biochem. 120 (1996) 946–953.

[28] N. Greenfield, G.D. Fasman, Computed Circular Dichroism Spectra for the Evaluation of Protein Conformation, Biochemistry 8 (1969) 4108–4116.

[29] Y. Xu, G. Feller, C. Gerday, N. Glansdorff. Moritella cold-active dihydrofolate reductase: Are there natural limits to optimization of catalytic efficiency at low temperature? J Bacteriol. 185 (2003) 5519–5526.

[30] D. Ishimaru, L.R. Andrade, L.S. Teixeira, P.A. Quesado, L.M. Maiolino, P.M. Lopez, Y. Cordeiro, L.T. Costa, W.M. Heckl, G. Weissmüller, D. Foguel, J.L. Silva, Fibrillar aggregates of the tumor suppressor p53 core domain. Biochemistry 42 (2003) 9022–9027.

[31] D. Ishimaru, L.M. Lima, L.F. Maia, P.M. Lopez, A.P. Ano Bom, A.P. Valente, J.L. Silva, Reversible aggregation plays a crucial role on the folding landscape of p53 core domain. Biophys. J. 87 (2004) 2691–2700.

[32] K. Hata, R. Kono, M. Fujisawa, R. Kitahara, Y.O. Kamatari, K. Akasaka, Y. Xu. High pressure nmr study of dihydrofolate reductase from a deep-sea bacterium *Moritella*

profunda, Cell Mol. Biol. (Noisy-le-grand) 50 (2004) 311–316.

[33] G. Dreyfus, H. Guimaraes-Motta, J.L. Silva, Effect of hydrostatic pressure on the mitochondrial ATP synthase. Biochemistry 27 (1988) 6704–6710.

[34] W. Kauzmann, Some factors in the interpretation of protein denaturation, Adv. Protein Chem. 14 (1959) 1–63.

[35] E. Ohmae, C. Murakami, K. Gekko, C. Kato, Pressure effects on enzyme functions, J. Biol. Macromol. 7 (2007) 23–29.

[36] R. Fraczkiewicz, W. Braun, Exact and efficient analytical calculation of the accessible surface areas and their gradients for macromolecules, J. Comp. Chem. 19 (1998) 319–333.

Figure Legends

Figure 1: **Superimposed drawing of the crystal structure of mpDHFR (black) and ecDHFR (gray) in the ternary complex with $NADP^+$ and folate.** PDB IDs for mpDHFR and ecDHFR are 2zza and 1rx2, respectively [4]. The figure was drawn using PyMol [http://www.pymol.org/].

Figure 2: **SDS-PAGE of ecDHFR and mpDHFR.** Lane 1: molecular weight markers; lanes 2 and 3: whole protein extracts from *E. coli* transformants overexpressing ecDHFR and mpDHFR, respectively; lanes 4 and 5: purified ecDHFR and mpDHFR, respectively; Acryl amide concentration of the gel was 15%.

Figure 3: **Far-ultraviolet CD (A) and fluorescence (B) spectra of ecDHFR and mpDHFR at pH 8.0 and 15 ºC.** The solvent used was 20 mM Tris-hydrochloride containing 0.1 mM EDTA and 0.1 mM dithiothreitol. Thin solid line: ecDHFR without ligands; thick solid line: mpDHFR without ligands; thick dashed line: mpDHFR with NADPH; and thick dash-dot line: mpDHFR with dihydrofolate.

Figure 4: **Pressure dependence of relative enzyme activity (A) and activation free energy (B) of ecDHFR and mpDHFR at 25 ºC and pH 7.0.** The solvent used was 20 mM

Tris-hydrochloride containing 0.1 mM EDTA, 0.1 mM dithiothreitol, 250 μM NADPH, and 250 μM dihydrofolate. Filled circle: ecDHFR (data from Murakami *et al*. [10]); open circle: mpDHFR. Solid lines in panel B were drawn by least-squares linear regression. Error bars represent the mean error of duplicate measurements.

Figure 5: **Temperature dependence of the far-ultraviolet CD spectra of ecDHFR (A) and mpDHFR (B) at pH 8.0.** The protein concentrations were 10 μM. Inset of panel B shows temperature dependence of the molar ellipticity at 222 nm for ecDHFR and mpDHFR.

Figure 6: **Pressure dependence of the center of fluorescence spectral mass (*CSM*) of ecDHFR (A) and mpDHFR (B) at pH 8.0 and various temperatures.** The proteins were equilibrated for 30 min (10 min for mpDHFR at 28.8 ºC only) at each pressure before the fluorescence spectra were measured. **Panel A**: Filled circle, 15.2 ºC; open circle, 20.4 ºC; and filled triangle, 27.0 ºC. **Panel B**: Filled circle, 15.7 ºC; open circle, 20.4 ºC; and filled triangle, 28.8 ºC. Solid lines represent the theoretical fit to a two-state unfolding model with the parameter values shown in Table 2. The insets show the pressure dependence of the apparent Gibbs free energy change due to unfolding (ΔG_u).

Figure 7: **Urea concentration dependence of the molar ellipticity at 222 nm (A) and the center of fluorescence spectral mass (*CSM*) (B) at 25 ºC and pH 8.0.** Filled and open circles indicate ecDHFR. Filled and open triangles indicate mpDHFR. Solid lines represent the theoretical fit to a two-state unfolding model with the parameter values shown in Table 3. Inset of panel B shows the urea concentration dependence of the apparent Gibbs free energy change due to unfolding (ΔG_u).

Figure 8: **Urea concentration dependence of the center of fluorescence spectral mass (*CSM*) of ecDHFR (A) and mpDHFR (B) at 25 ºC and pH 8.0 under various pressures.** The proteins were equilibrated for 24 h at each denaturant concentration for 10 min at each pressure before the spectra were measured. Filled circle: 0.1 MPa; open circle: 50 MPa; filled triangle: 100 MPa; open triangle: 150 MPa; filled square: 200 MPa; and open square: 250 MPa. Solid lines represent the theoretical fit to a two-state unfolding model with the parameter values shown in Table 3. Inset of panel B shows the pressure dependence of the Gibbs free energy change due to unfolding in the absence of urea (ΔG°_U). Solid and open circles represent ecDHFR and mpDHFR, respectively. Solid lines were drawn by least-squares linear regression.

Table 1: **Activation volumes for enzyme function of ecDHFR and mpDHFR at 25 °C and pH 7.0** [a]

	ΔV^* / ml mol^{-1} [b]	
ecDHFR [c]	7.5±0.2 (0.1–225 MPa)	
mpDHFR	−8.6±2.5 (0.1–50 MPa)	8.6±0.9 (50–200 MPa)

[a] Solvent used was 20 mM Tris-hydrochloride containing 0.1 mM EDTA, 0.1 mM dithiothreitol, 250 μM NADPH, and.250 μM DHF.

[b] Values in parentheses indicate the pressure range used for calculation.

[c] Murakami *et al*. [10].

Table 2: **Thermodynamic parameters for pressure unfolding of ecDHFR and mpDHFR at various temperatures** [a]

	Temperature / °C	$\Delta G°_P$ / kJ mol^{-1}	ΔV_P / ml mol^{-1}	P_m / MPa
ecDHFR	15.2	16.5 ± 1.4	−64 ± 6	258 ± 33
	20.4	20.0 ± 2.6	−74 ± 11	270 ± 53
	27.0	21.5 ± 1.5	−79 ± 6	272 ± 30
mpDHFR	15.7	3.3 ± 0.4	−50 ± 3	66 ± 9
	20.4	3.3 ± 0.3	−49 ± 3	67 ± 7
	28.8	2.9 ± 0.2	−40 ± 2	73 ± 6

[a] Solvent used was 20 mM Tris-hydrochloride (pH 8.0) containing 0.1 mM EDTA and 0.1 mM dithiothreitol.

Table 3: **Thermodynamic parameters for urea unfolding of ecDHFR and mpDHFR at 25 °C under various pressures** [a]

	Method	Pressure / MPa	$\Delta G°_U$ / kJ mol^{-1}	m / kJ mol^{-1} M^{-1}	C_m / M	ΔV_U / ml mol^{-1}
ecDHFR	CD	0.1	22.5 ± 2.3	9.0 ± 0.9	2.5 ± 0.4	
	Fluorescence	0.1	21.8 ± 1.8	8.2 ± 0.7	2.7 ± 0.3	−85 ± 7
		50	19.4 ± 1.5	9.3 ± 0.7	2.1 ± 0.2	
		100	12.6 ± 0.4	8.0 ± 0.2	1.6 ± 0.1	
		150	7.8 ± 0.3	7.0 ± 0.3	1.1 ± 0.1	
		200	4.2 ± 0.3	5.7 ± 0.2	0.7 ± 0.1	
		250	2.0 ± 0.0	4.8 ± 0.1	0.4 ± 0.0	
mpDHFR	CD	0.1	7.6 ± 0.8	4.8 ± 0.5	1.6 ± 0.2	
	Fluorescence	0.1	7.9 ± 0.6	4.3 ± 0.2	1.8 ± 0.2	−53 ± 7
		50	4.2 ± 0.1	4.3 ± 0.1	1.0 ± 0.0	
		100	1.4 ± 0.1	3.5 ± 0.1	0.4 ± 0.0	
		150	0.0 ± 0.1	2.9 ± 0.1	0.0 ± 0.0	
		200	ND [b]	ND	ND	
		250	ND	ND	ND	

[a] Solvent used was 20 mM Tris-hydrochloride (pH 8.0) containing 0.1 mM EDTA and 0.1 mM dithiothreitol.

[b] Not determined.

Figure 1: E. Ohmae *et al.*

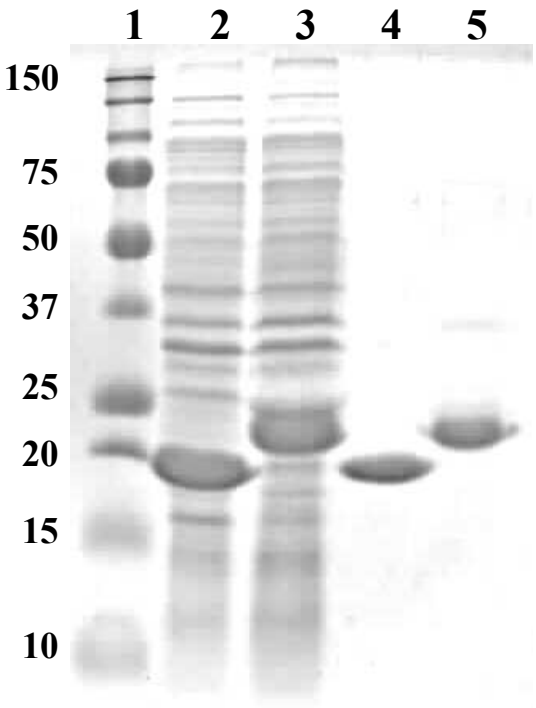

Figure 2: E. Ohmae *et al.*

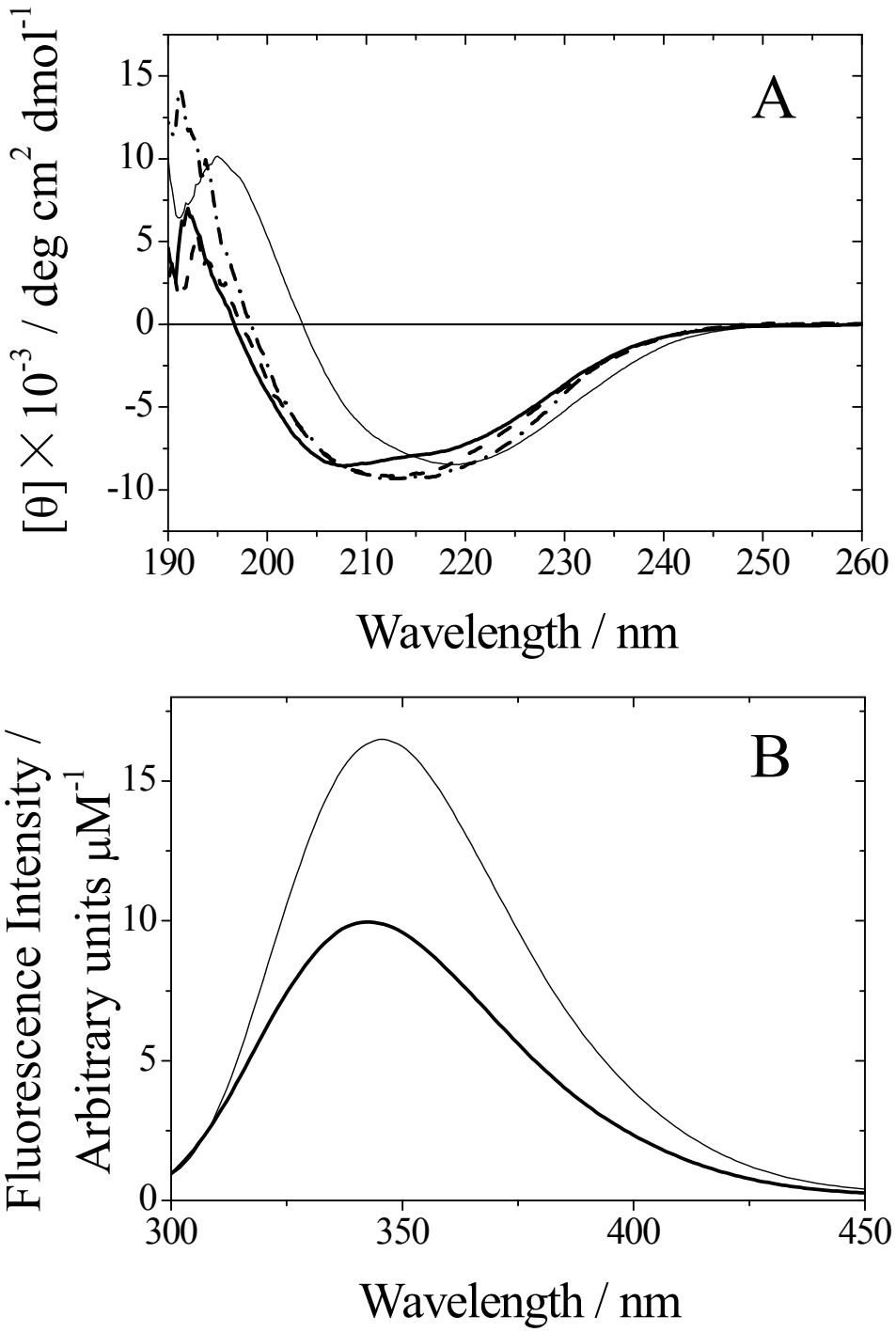

Figure 3: E. Ohmae *et al.*

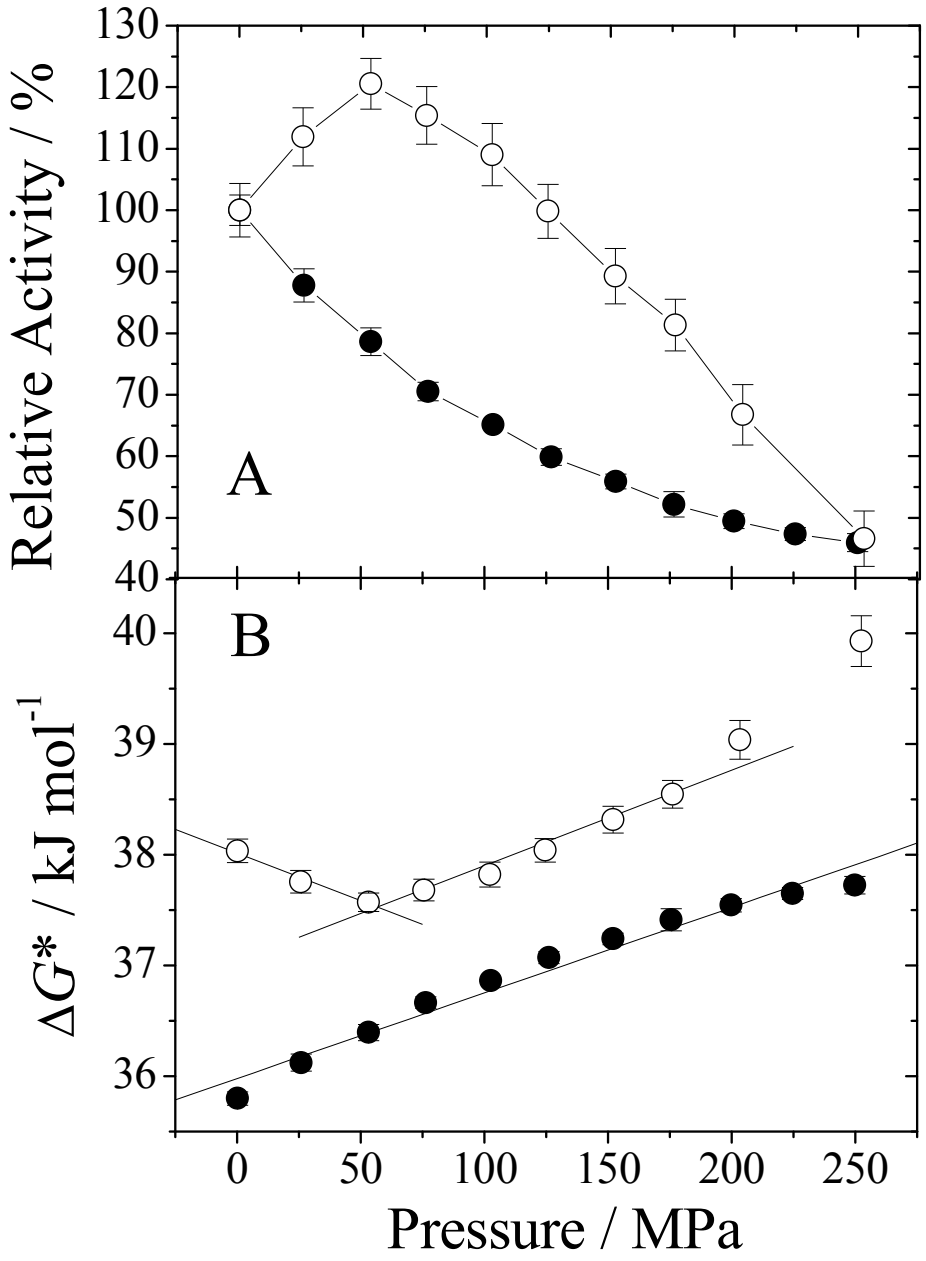

Figure 4: E. Ohmae *et al.*

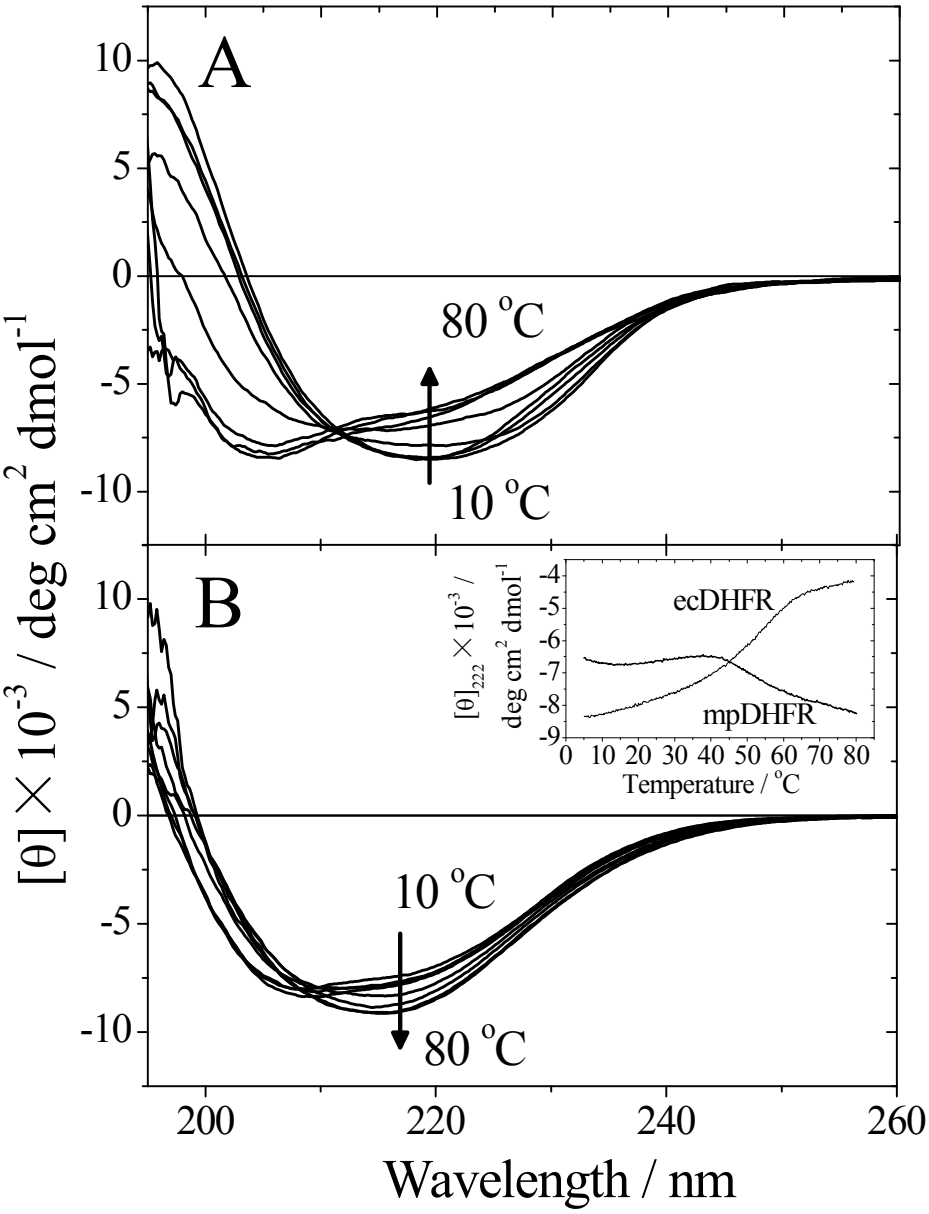

Figure 5: E. Ohmae *et al.*

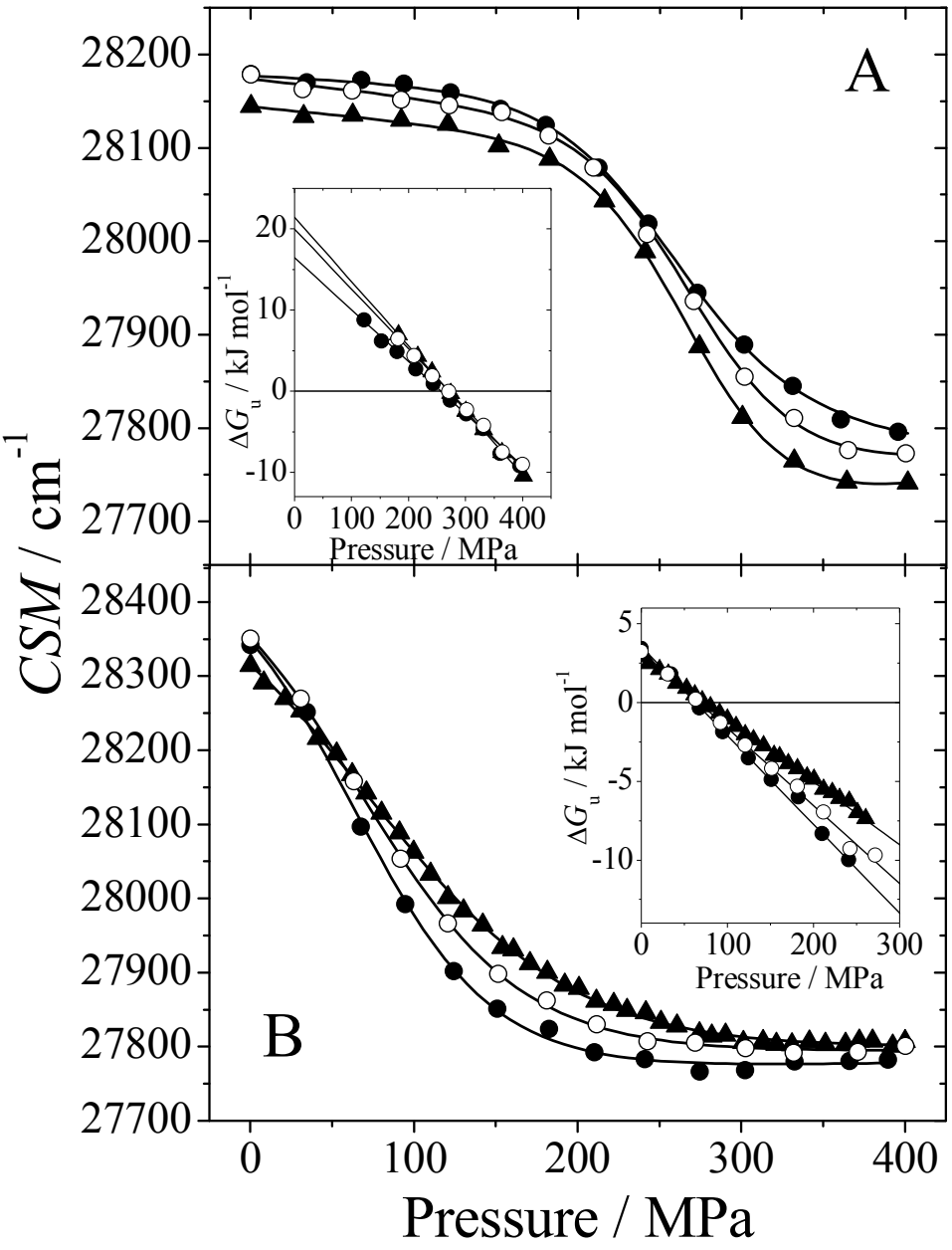

Figure 6: E. Ohmae *et al.*

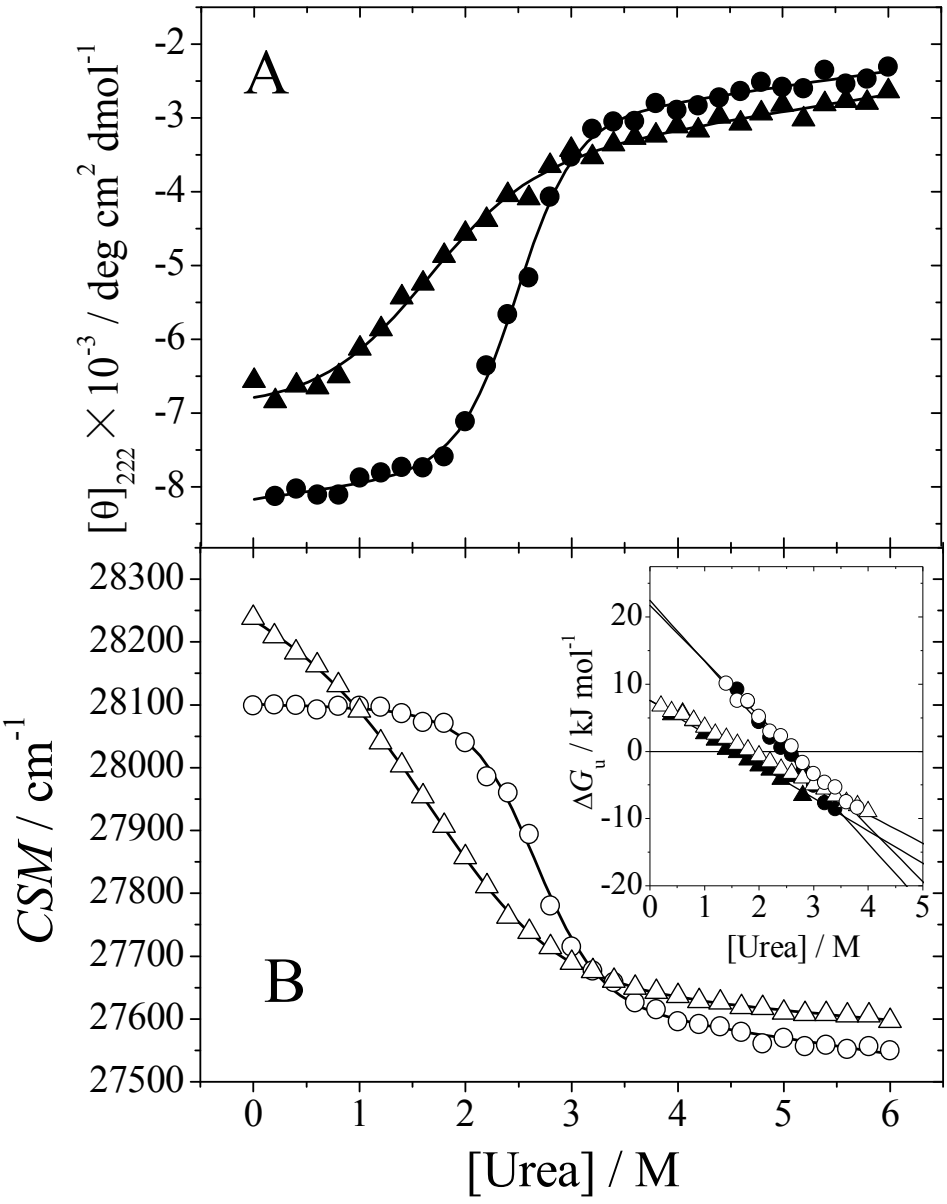

Figure 7: E. Ohmae *et al.*

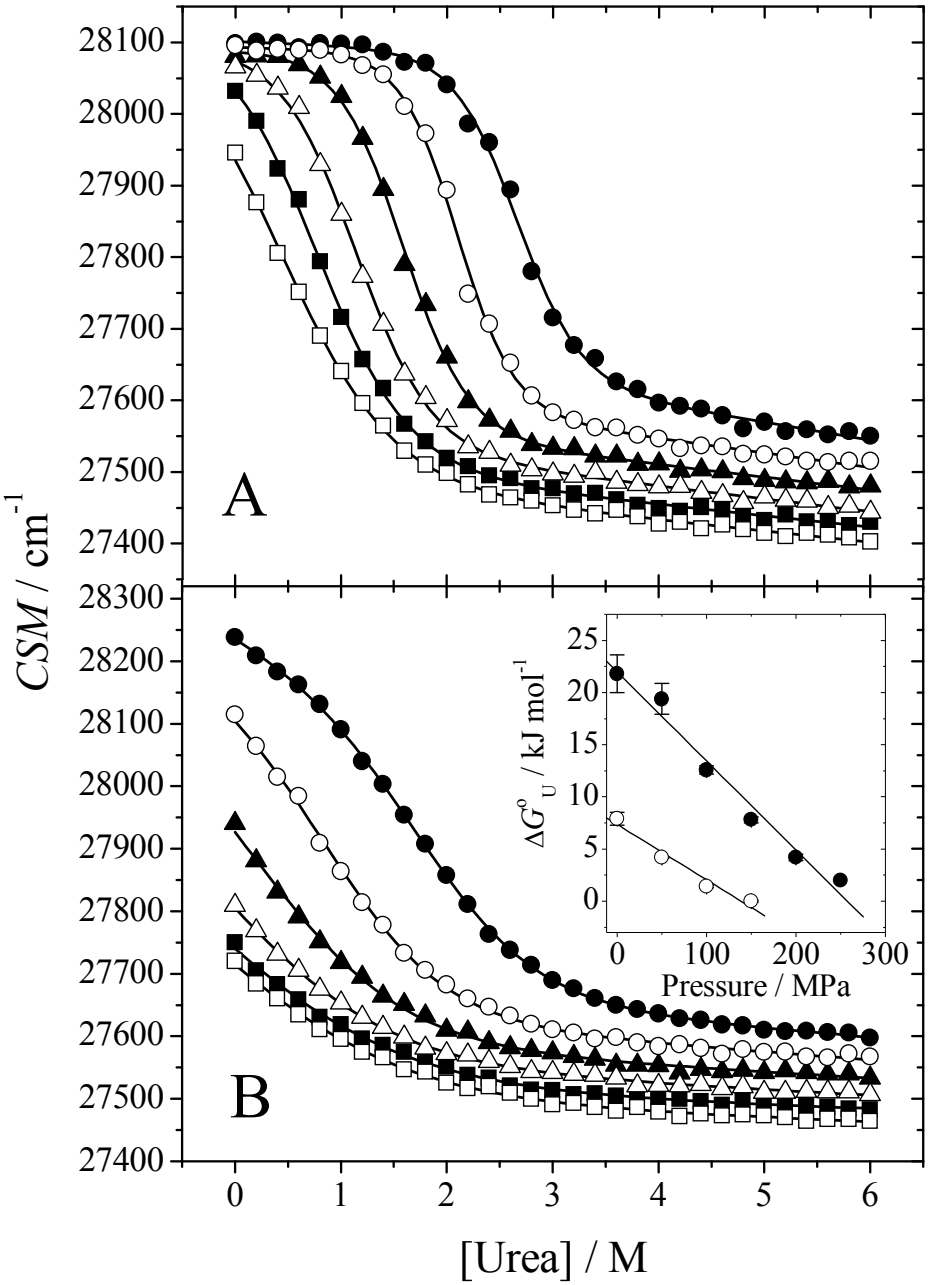

Figure 8: E. Ohmae *et al.*

Pressure Dependence of Activity and Stability of Dihydrofolate Reductases of the Deep-sea Bacterium *Moritella profunda* and *Escherichia coli*

Supplementary Figures

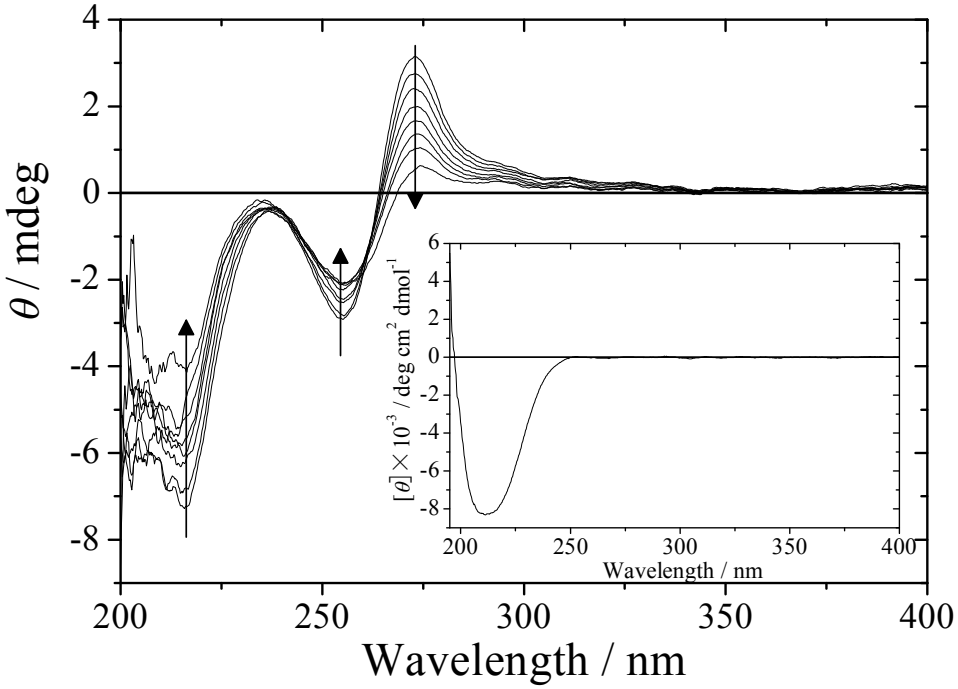

Figure S1: **Temperature dependence of the CD spectrum of $NADP^+$ at pH 8.0.** Arrows indicate the direction of the spectral change with increasing temperature from 10 to 80 ºC. The solvent used was 20 mM Tris-hydrochloride containing 0.1 mM EDTA and 0.1 mM dithiothreitol. The concentration of $NADP^+$ was 0.5 mM using a 1-mm path length cell. Inset shows far- and near-ultraviolet CD spectrum of mpDHFR without ligands at 25 ºC and pH 8.0.

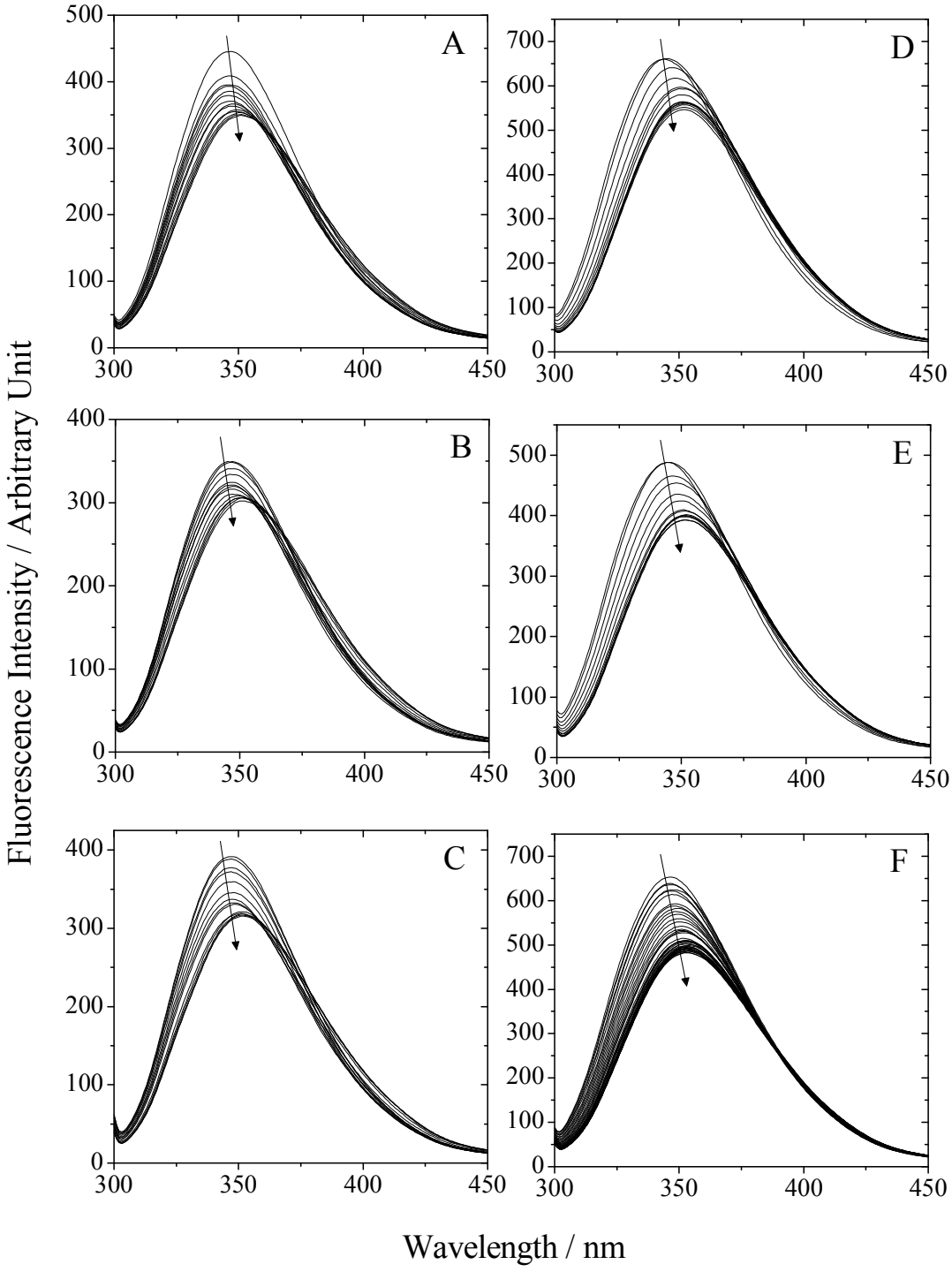

Figure S2: **Pressure dependence of the fluorescence spectra of ecDHFR and mpDHFR at pH 8.0.** (A) ecDHFR at 15.2 ºC, (B) ecDHFR at 20. 4 ºC, (C) ecDHFR at 27.0 ºC, (D) mpDHFR at 15.7 ºC, (E) mpDHFR at 20.4 ºC, and (F) mpDHFR at 28.8 ºC. Arrows indicate the direction of the spectral change from 0.1 to 400 MPa. The solvent used was 20 mM Tris-hydrochloride containing 0.1 mM EDTA and 0.1 mM dithiothreitol.

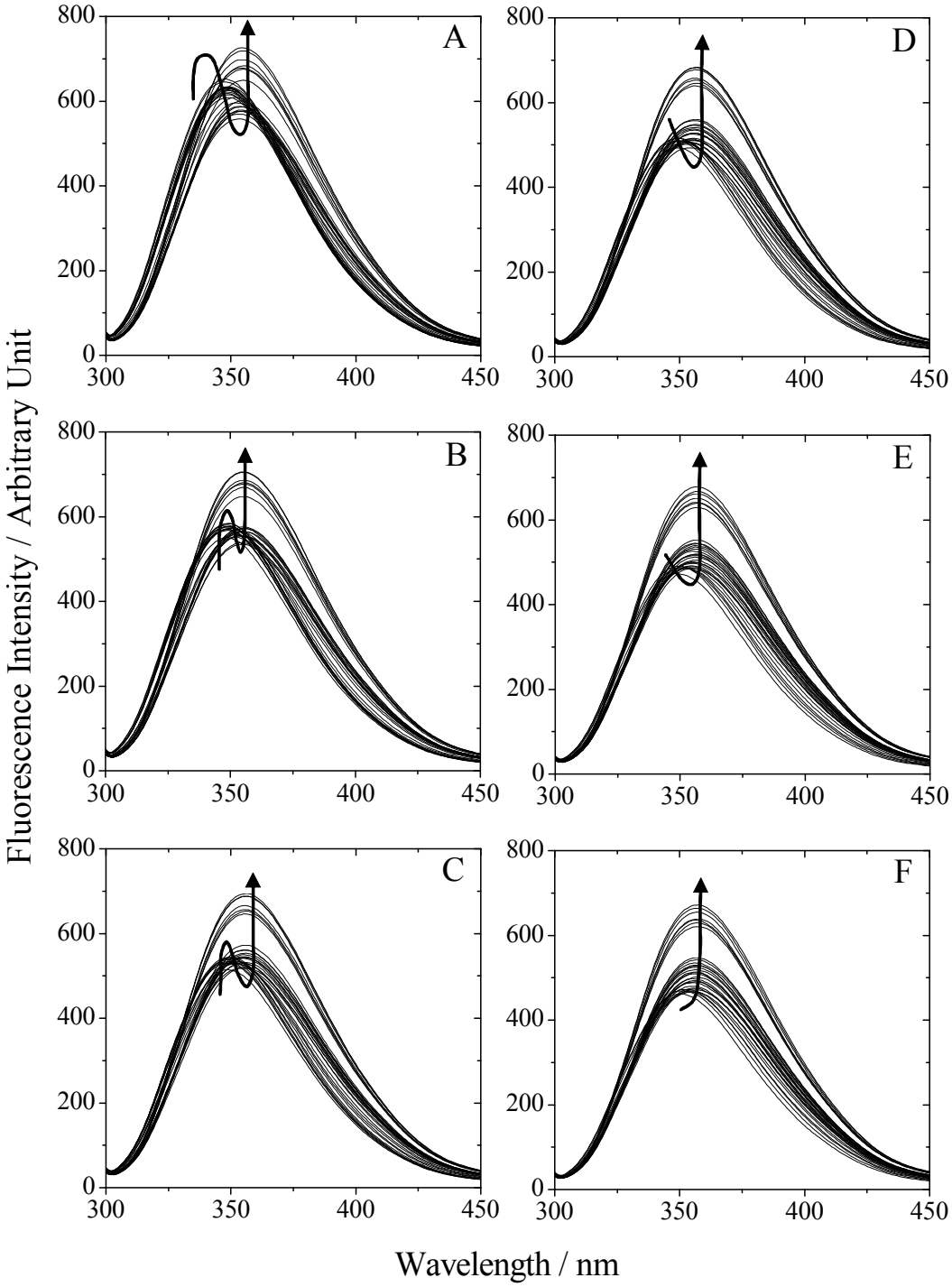

Figure S3: **Urea concentration dependence of the fluorescence spectra of ecDHFR at 25 ºC and pH 8.0.** (A) 0.1 MPa, (B) 50 MPa, (C) 100 MPa, (D) 150 MPa, (E) 200 MPa, and (F) 250 MPa. Arrows indicate the direction of spectral change with increasing urea concentration from 0 to 6 M. The solvent used was 20 mM Tris-hydrochloride containing 0.1 mM EDTA and 0.1 mM dithiothreitol. Note that the center of fluorescence spectral mass is independent of the protein concentration.

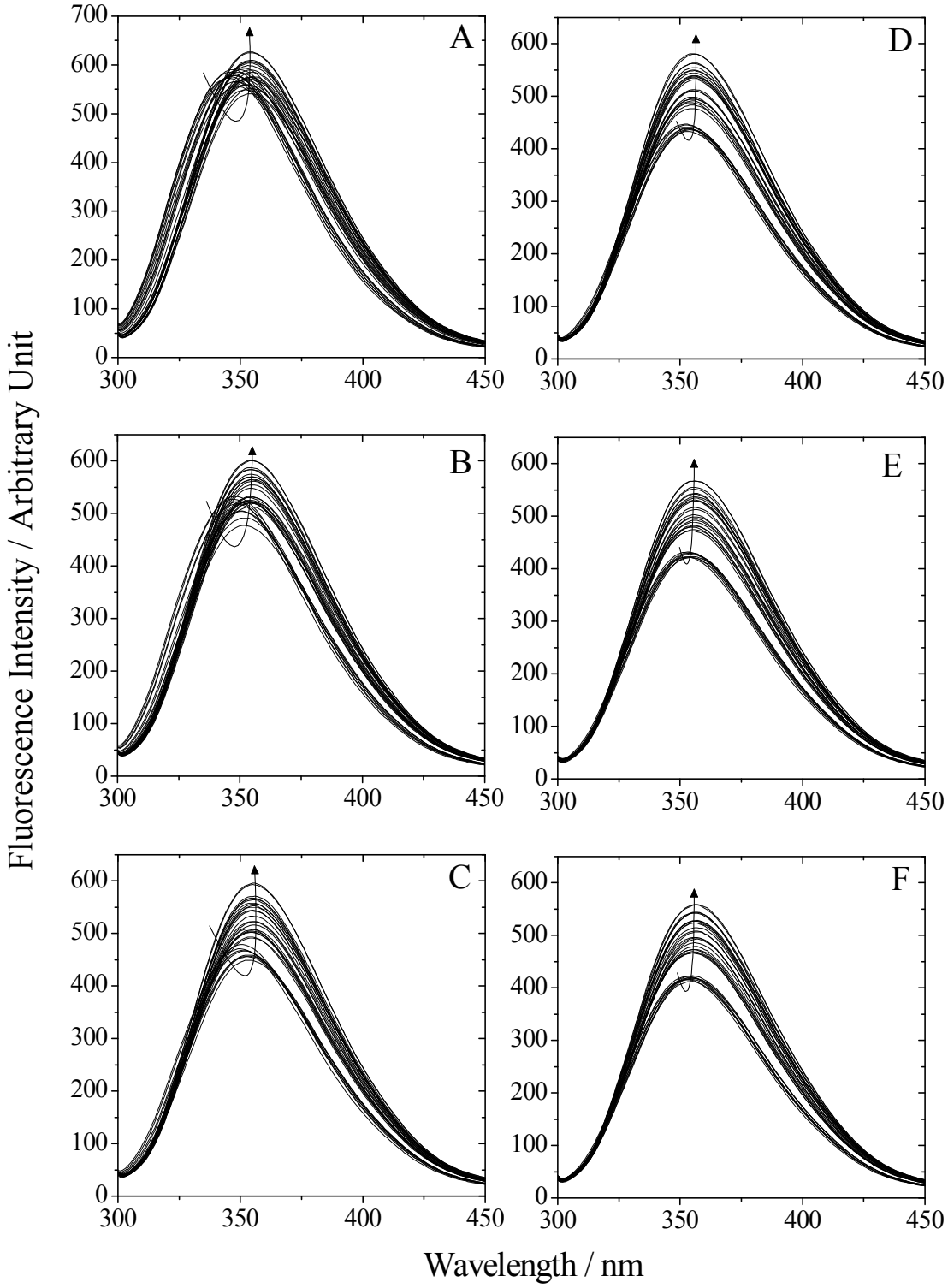

Figure S4: **Urea concentration dependence of the fluorescence spectra of mpDHFR at 25 ºC and pH 8.0.** (A) 0.1 MPa, (B) 50 MPa, (C) 100 MPa, (D) 150 MPa, (E) 200 MPa, and (F) 250 MPa. Arrows indicate the direction of spectral change with increasing urea concentration from 0 to 6 M. The solvent used was 20 mM Tris-hydrochloride containing 0.1 mM EDTA and 0.1 mM dithiothreitol.